Exploratory Analysis of Nonuniform Plug Nozzle Flowfields

CHARLES R. HALL JR.* AND THOMAS J. MUELLER†
University of Notre Dame, Notre Dame, Ind.

A method is presented by which the plug nozzle flowfield is calculated for the "closed wake" condition. The assumed flow model is divided into two basic components: the separated region or near wake and the inviscid flow adjacent to this near wake. The solution to the near wake is obtained by means of an integral analysis, and the rotational method of characteristics solution is employed in the adjacent inviscid region. Parametric studies for representative nozzle configurations are also included. These parameters include the effects of: plug truncation for an internal-external-expansion truncated plug nozzle, shroud truncation for an expansion-deflection nozzle, the over-all nozzle area ratio, nonisoenergetic mixing, the variation of the ambient pressure, base bleed, and boundary-layer thickness approaching separation. Comparison with a limited amount of experimental data is also presented.

Nomenclature

A = area
H = nondimensional bleed number, Refs. 1, 5 or 6
L = plug length measured from geometric throat
M = Mach number
$\dot{m}$ = mass flow rate
n = power law profile exponent
P = pressure
r = radius
T = temperature
u = velocity
X,Y = coordinates of the reference (inviscid) coordinate system
x,y = coordinates of the intrinsic (viscous) coordinate system
γ = ratio of specific heats
δ = boundary-layer thickness
δ^{**} = boundary-layer momentum thickness
ε = 0 for planar flows; = 1 for axisymmetric flows
η = dimensionless coordinate ($=\sigma y/x$)
θ = streamline angle
ρ = density
σ = jet spread parameter
ϕ = velocity ratio, u/u_1

Subscripts

1,2,3,4 = stations for the basic flow model
a = conditions in the external stream adjacent to the mixing region; ambient conditions
an = analytical
b = conditions at the plug base
BL = boundary layer
d = streamline whose kinetic energy is just sufficient to enter the recompression region
E = nozzle exit
exp = experimental
j = conditions along the jet boundary separating streamline
m = coordinate shift in the mixing theory due to the momentum integral
max = maximum
o = stagnation conditions
R = conditions along the R-streamline
t = nozzle throat
w = wake

Superscripts

$-$ = average value

Presented as Paper 71-41 at the AIAA 9th Aerospace Sciences Meeting, New York, N.Y., January 25–27, 1971; submitted March 19, 1971; revision received December 6, 1971. Research supported by NASA under Contract NSR 15-004-029 and the Department of Aerospace and Mechanical Engineering, and was part of the Ph.D. dissertation of the first author. The authors gratefully acknowledge the efforts of H. Ackert for preparing the figures and A. E. Fanning, F. L. Galanga, and T. V. Giel for their helpful comments in preparing this manuscript.

Index categories: Electric and Advanced Space Propulsion; Subsonic and Supersonic Airbreathing Propulsion; Jets, Wakes, and Viscid-Inviscid Flow Interactions.

* Research Assistant. Member AIAA.
† Professor. Associate Fellow AIAA.

Introduction

FOR certain atmospheric and space missions, propulsive systems are required which provide large thrust-to-weight ratios, and also perform efficiently over a wide range of operating conditions. Plug nozzle configurations such as the expansion-deflection (*E-D*) and the truncated plug (*T-P*) may provide the means for satisfying these requirements. Schematics of these geometries are pictured in Figs. 1a and 1b, respectively. These nozzles are much shorter than the corresponding bell or conical nozzles of the same over-all area ratio. In addition, these nozzles have an altitude compensating capability because their flowfields adjust to the ambient conditions, thus producing a more efficient operation at off-design altitudes. In order to develop design criteria for such nozzles, analytical techniques must be developed which describe the flowfield accurately. A basic flow model is extended to analyze these nozzle geometries. Also included is a discussion of the influence of representative parameters along with a limited amount of experimental data.

Basic Flow Model

Although the flow between the near wake and the external jet boundary is assumed to be inviscid, it may be rotational. The method of characteristics solution proceeds downstream from the initial line, and portions of the flowfield which have already been determined cannot be affected by conditions downstream. The near wake-base pressure solution determines the lower boundary condition for the method of characteristics solution. On the other hand, the method of characteristics solution provides the boundary condition for the near wake solution (Fig. 1).

The shape of the base flow region downstream of the plug is determined by employing an extension of the flow model developed by Zumwalt[1] and later modified by Mueller.[2,3] Besides calculating the plug base pressure, the general features of the entire nozzle flowfield are obtained. The theoretical flow model used in conjunction with the restricted mixing theory of Korst[4] and the rotational method of characteristics is shown in Fig. 2. The flow is divided into an inviscid adjacent stream, a dissipative mixing layer, and a base region.

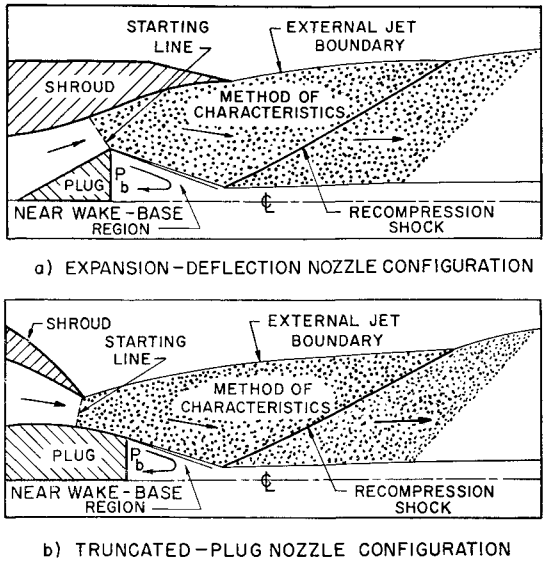

Fig. 1 Essential features of "closed wake" plug nozzle flowfields.

In addition to using the restricted mixing theory of Korst, the following conditions are imposed on these three flow components. 1) The initial conditions in the throat of the nozzle may be either along a left-running characteristic (as in an *E-D* nozzle), along a right-running characteristic (as in a *T-P* nozzle), or along a noncharacteristic line. The flow need not be uniform at this initial condition line, but must be supersonic. Adjacent nozzle flow is calculated using the rotational method of characteristics. 2) The boundary layer approaching the separation corner at 1 is neglected, although the mixing is assumed to be fully turbulent (after Korst[4] and Zumwalt[1, 5]). 3) An isentropic expansion takes place in the adjacent stream from 1 to 2, i.e., a continuation of the method of characteristics for the flow over the plug. The presence of a lip shock is ignored in this analysis. 4) The inviscid flow past a conetail using the rotational method of characteristics is utilized to define the pressure field impressed on the mixing region from 2 to 3. This conetail surface also serves as the "corresponding inviscid jet boundary". 5) The pressure normal to the "corresponding inviscid jet boundary" is assumed to be constant within and near the mixing region at each cross-section (after Zumwalt[1, 5] and Mueller[2, 4]). 6) Velocity profile similarity is assumed in the mixing region. The error function velocity distribution is located within the intrinsic coordinates x, y and is represented by $x \approx X$ and $Y = y\text{-}y_m(x)$ where $y_m(0) = 0$. This coordinate shift is a consequence of using the restricted mixing theory of Korst (after Korst,[4] Zumwalt[1, 5] and Mueller [2, 3]). 7) Recompression is assumed to result from an oblique shock turn from 3 to 4 at an empirically determined trailing wake radius ratio (after Mueller[2, 3]).

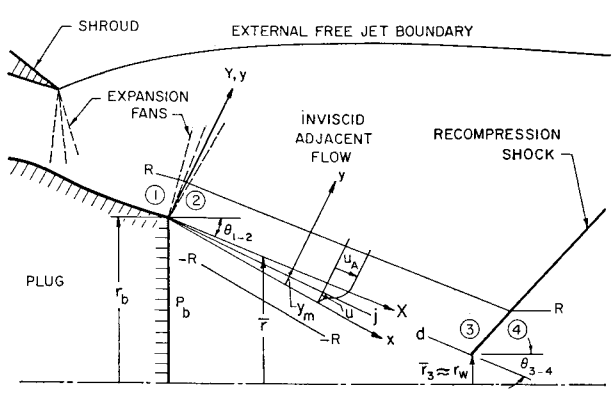

Fig. 2 Flow model used to determine the turbulent base pressure and flowfield for a plug nozzle.

A streamline j can be identified which divides the amount of mass passing over the corner at 1 from that mass flow entrained by the viscous action of the free jet mixing region. A second streamline d can be identified which has just sufficient kinetic energy at 3 to negotiate the pressure rise to 4. Streamlines below the d-streamline have lower kinetic energies, cannot pass through recompression, and are turned back to recirculate in the base region. If there is no base bleed, conservation of mass requires that the j- and d-streamlines be identical.

The control volume between cross sections 2 and 3 is bounded by streamlines R and $-R$ which were defined by Zumwalt[1] such that the cross-sectional area normal to the direction of the flow would remain nearly constant, and the $P \cdot dA$ pressure force could be neglected in the momentum equation. The momentum equation in the axial direction was formulated using geometrical relations and the relationship between the viscous and inviscid coordinate systems. This equation was solved simultaneously with the combined viscous and inviscid continuity equations written for the control volume between cross sections 2 and 3. For the error function velocity profile, $\phi = \frac{1}{2}(1 + \text{erf}\ \eta)$, where $\phi = u/u_a$ and $\eta = \sigma y/x$, it was found that $\eta_R = 3$ was large enough for ϕ_j to approach its asymptotic value. The result of this analysis is a nonlinear equation which allows one to locate the j-streamline at cross section 3. (Refs. 1–3 and 6 give details of the analysis.)

It is evident that, in order to determine η_{j3} and therefore ϕ_{j3} for a given initial condition, the location of recompression, $\bar{r}_3/r_b$, the corresponding inviscid condition M_{3a}, and the jet spread parameter, σ_{3a}, must be known. The location of the recompression point, $\bar{r}_3/r_b$, is determined from experimental data. The Mach number along the inviscid jet boundary at 3, M_{3a}, is determined from the axisymmetric rotational method of characteristics solution. The jet spread parameter is determined from the equation given by Channapragada.[7]

In considering base flows in which base bleed (i.e., mass addition) is present, modifications of flow model must be made. Additional assumptions include: a) the amount of mass addition is small; b) the momentum associated with this mass addition is negligible; and c) for steady mass bleed cases, some amount of mass will be pumped into or out of the base region through the mixing region between the j- and d-streamlines. The analysis of base bleed used here is that of Zumwalt and Tang.[5]

The initial boundary layer approaching separation is treated as an equivalent base bleed.[8-10] The actual amount of equivalent base bleed due to the finite boundary layer $\dot{m}_{BL}$ may be expressed as: $\dot{m}_{BL} = 2\rho_1 u_1 \delta^{**}(\pi r_{BL})^{\epsilon}$. In this analysis, the boundary-layer profile approaching the end of the plug has been assumed to take the form given by a power law expression, i.e.: $u/u_1 = (y/\delta)^{1/n}$.

FORTRAN IV programs for the UNIVAC 1107 digital computer were developed to calculate the flowfields and base pressures for axisymmetric and planar *E-D* and *T-P* nozzle configurations.

Analytical Studies

A supersonic starting line must be determined which forms the initial boundary conditions for the method of characteristics. Since the base pressure solution is a direct function of the characteristics solution, the base pressure, then, can provide a numerical comparison demonstrating the effects of an initial profile shape. Four types of profiles were investigated for an internal-external-expansion *T-P* nozzle: a) a vertical profile; b) a parabolic profile; c) a linear profile; and d) a circular arc profile. The initial Mach number for all four cases was 1.050, and the streamline angle varied linearly between the

plug surface and the contour surface. The lowest base pressure was obtained with the linear sonic line and the highest with the circular arc sonic line (i.e., about 29% higher than the linear sonic line). The values obtained for the vertical and parabolic sonic lines were essentially the same and about 17% higher than the linear case. The vertical sonic line was used in all of the cases presented below.

Truncating the shroud of an *E-D* nozzle may produce significant weight savings while keeping the thrust losses to a minimum. The effects of shroud truncation on the flowfield of an axisymmetric *E-D* nozzle are presented in Fig. 3. Although the amount of shroud truncation is not large (a maximum of 1.59% decrease in exit area in Fig. 3), rather significant changes in the flowfield are encountered. The most significant change in the flowfield occurs in the shape and location of the external free-jet boundary. The initial flow angle at the shroud exit increases with increasing truncation because the flow at the exit must undergo a larger expansion to the ambient pressure. The base pressure for all three cases remained constant since the effects of the truncated shroud had not propagated into the near wake region. The shape of the external jet boundary also governs the formation of the internal shock system. The internal shock is formed by a coalescence of compression waves originating at this boundary. This type of internal shock was not included in the analysis.

One technique used to produce higher thrust levels is to vary the nozzle area ratio, A_E/A_t. The nozzle used in this investigation was an internal-external-expansion *T-P* nozzle with a cylindrical shroud. The radius of the shroud was allowed to vary while the plug geometry remained constant. The results of this study are shown in Fig. 4. An increasing area ratio produces a corresponding decrease in the base pressure. Since the Mach number is directly related to the area ratio, this result, then, does produce the proper trend as demonstrated by many other authors.[2-4,11]

In hot flow nozzles, the base temperature (i.e., the gas temperature near the plug base) can differ greatly from the freestream stagnation temperature. With increasing time, the base temperature begins to approach this freestream stagnation temperature asymptotically. In the interim, however, the performance of the nozzle may vary appreciably. The solution presented here cannot predict the actual transient variation of the base pressure with the rate of increase (or decrease) of base temperature. The analysis can provide, however, a

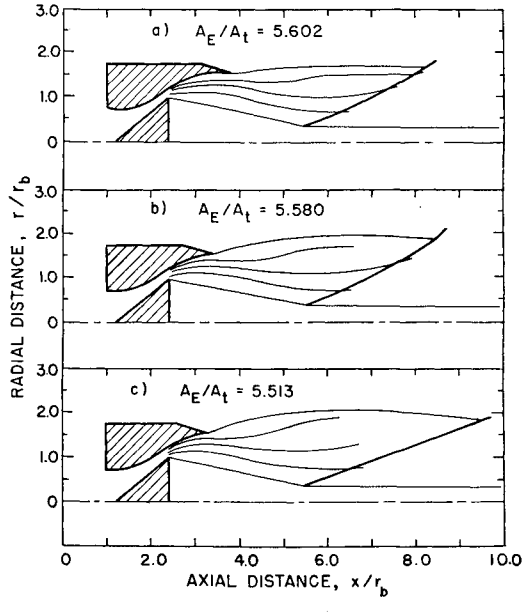

Fig. 3 Shroud contour truncation of an axisymmetric *E-D* nozzle with $A_b/A_t = 2.448$, $P_a/P_{o1} = 0.0102$, $H = 0$, $P_b/P_{o1} = 0.0219$, $T_b/T_{o1} = 1.00$, and $\gamma = 1.4$.

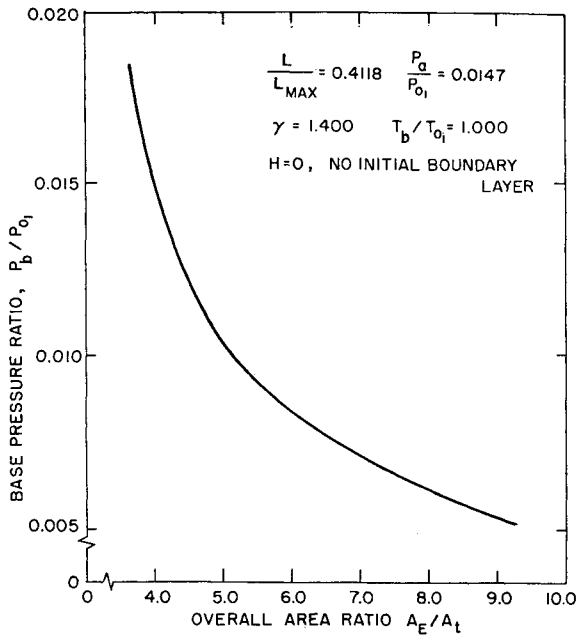

Fig. 4 Influence of area ratio on base pressure ratio for an axisymmetric internal-external-expansion truncated plug nozzle with a 7.97° half-angle conical plug.

representation of the flowfield providing the rate of temperature change is not too large. The results of nonisoenergetic mixing on the base pressure of an axisymmetric *E-D* nozzle are shown in Fig. 5. Note that the base pressure increases with heat addition, while cooling produces a base pressure decrease. This trend has been demonstrated both analytically and experimentally by other authors for simple base flow problems.[12-14]

Plug nozzles are altitude compensating because their flowfields change with changes in ambient pressures. For a *T-P* nozzle, the external free-jet boundary forms the upper boundary for the nozzle flow. The effects of ambient pressure on the flowfield of a planar *T-P* nozzle are shown in Fig. 6. In this figure, the increasing ambient pressure, from *a* to *c* forces the external free jet boundary toward the nozzle axis which results in significant changes in the nozzle flowfield (although the base region has not been affected for the cases shown in Fig. 6).

Mass addition into the near wake of a blunt body is an

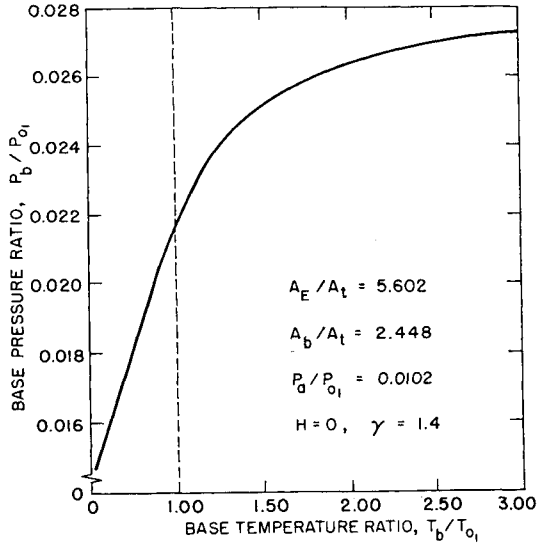

Fig. 5 Effect of nonisoenergetic mixing on the base pressure of an axisymmetric *E-D* nozzle.

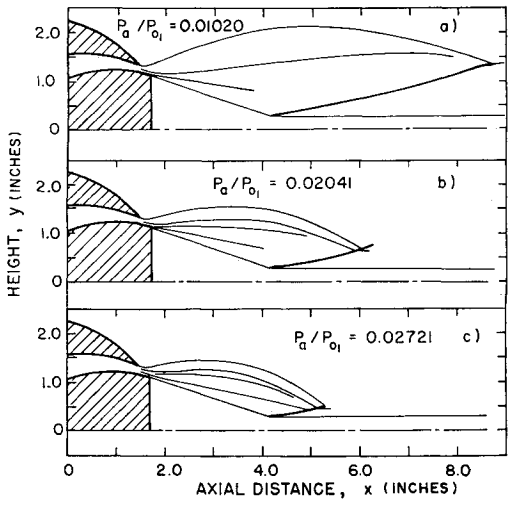

Fig. 6 Effect of ambient pressure on the flowfield of a planar *T-P* nozzle with $A_E/A_t = 15.573$, $A_b/A_t = 13.330$, $P_b/P_{o1} = 0.0733$, $H = 0$, $T_b/T_{o1} = 1.00$, and $\gamma = 1.4$.

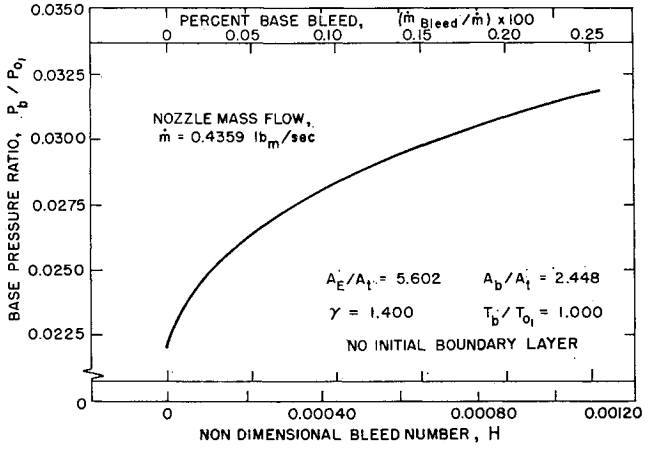

Fig. 7 Effect of base bleed on the base pressure of an axisymmetric *E-D* nozzle.

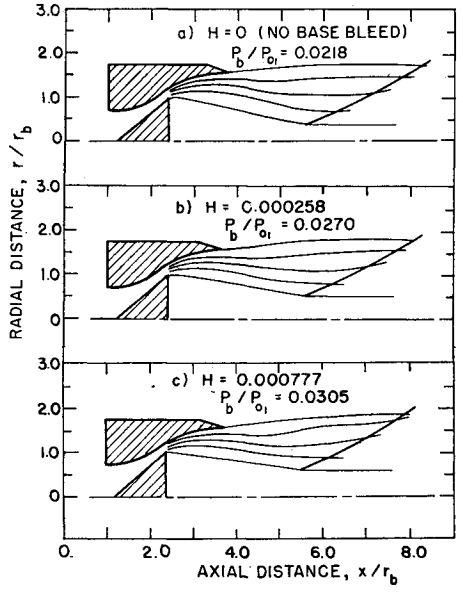

Fig. 8 Effects of base bleed on the flowfield of an axisymmetric *E-D* nozzle, with $A_E/A_t = 5.062$, $A_b/A_t = 2.448$, $T_b/T_{o1} = 1.00$ and $\gamma = 1.4$.

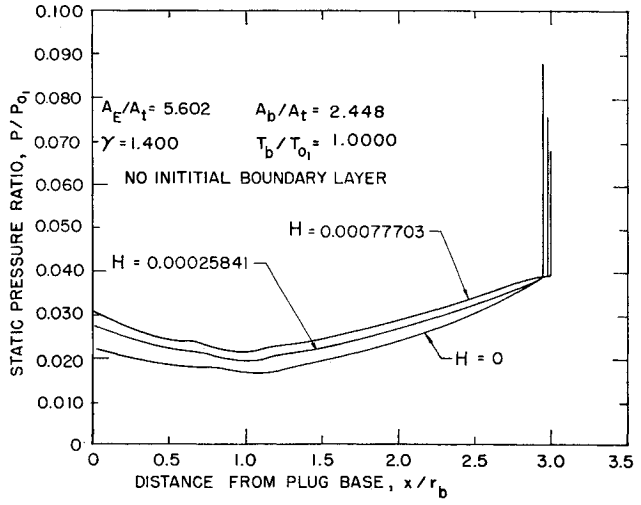

Fig. 9 Calculated pressure variations along the inviscid jet boundary of the near wake of an axisymmetric *E-D* nozzle.

effective means of substantially increasing the base pressure[12,15] which in turn, increases the total thrust of the nozzle. Figure 7 shows the effect of base bleed on the base pressure of an axisymmetric *E-D* nozzle, while Fig. 8 presents the calculated flowfields at three different bleed rates. Figure 7 demonstrates that initially, the effect on base pressure is quite large, but begins to level off with increasing bleed rates. In Fig. 8, the flowfields also reflect this change in the base pressure. Recompression was made to occur at a larger radius, and the axial location of recompression was shifted slightly downstream.[6] Figure 9 presents the static pressure variation along the near wake up to and including recompression for the three cases of Fig. 8. Note that the curve for no base bleed has the lowest base pressure, while increasing bleed rates produce higher base pressures. At recompression, the pressures are all approximately the same value, but the

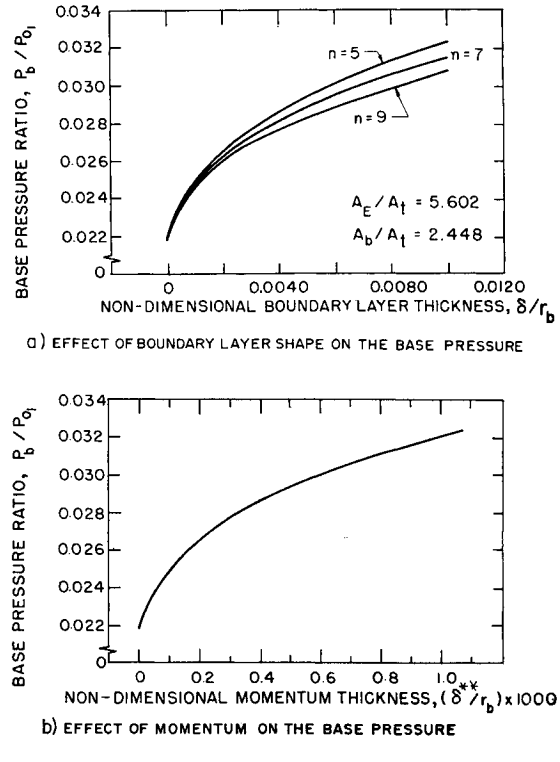

Fig. 10 Initial boundary-layer effects on the base pressure of an axisymmetric *E-D* nozzle with $P_a/P_{o1} = 0.0102$.

pressure rise across the recompression shock is not as great for the bleed cases.

An initial boundary layer just upstream of separation may be treated as an equivalent base bleed.[8-10] Therefore, the flowfield and base pressure of a nozzle will be influenced by the presence of an initial boundary layer. Figure 10 presents the effects of a turbulent boundary layer on the base pressure of an axisymmetric *E-D* nozzle. The variations in base pressure with the velocity profile exponent are presented in Fig. 10a. Figure 10b presents the variation of the base pressure with the nondimensional momentum thickness of the initial boundary layer. Since the momentum thickness is directly proportional to the equivalent base bleed, this curve is identical to the base bleed curve for the same nozzle (Fig. 7).

Experimental Studies

An internal-external-expansion nozzle was designed for an exit Mach number of 1.90 based on the over-all area ratio, $A_E/A_t = 1.555$. The plug was conical in shape and converged toward the axis at an angle of 10°; and the base was 0.48 of the distance from the throat to the projected cone tip (i.e., $L/L_{max} = 0.48$). The base diameter was 0.250 in., the length of the truncated plug from the throat was 0.660 in., and the nozzle throat area was 0.33 in.^{2}. The shroud contour of the nozzle was cylindrical and extended a distance of 0.300 in. downstream of the geometric throat. A more complete description of the nozzle and its auxiliary equipment is given in Ref. 6.

The calculated near wake boundary and recompression shock as well as the external free jet boundary were compared with the results obtained from a shadowgraph of this flowfield in Fig. 11. The calculated external free jet boundary agreed very well with the experimental one. The near wake boundary and recompression shock did not agree as well. This was anticipated because of the difference in the calculated ($P_b/P_{o1} = 0.0878$) and measured ($P_b/P_{o1} = 0.0693$) values of base pressure ratio. Although the use of a vertical sonic line and omission of the plug boundary layer in the analytical model could account for some of the difference, it appears that the omission of an internal shock wave in the calculations would explain more of the discrepancy.

Additional comparisons with a small amount of unpublished data[16] were also made. No internal shock waves were apparent in the shadowgraphs from these experiments. The nozzle was an internal-external-expansion *T-P* nozzle with $A_E/A_t = 24$, the diameter of the cylindrical shroud was 3.00 in. and the diameter of the plug at the throat was 2.937 in. The shroud of the nozzle extended a distance of 1.180 in. downstream of the throat. The plug had a cone half-angle of 17° and was truncated at three lengths for the experiments. A comparison of the analytical and experimental base pressures

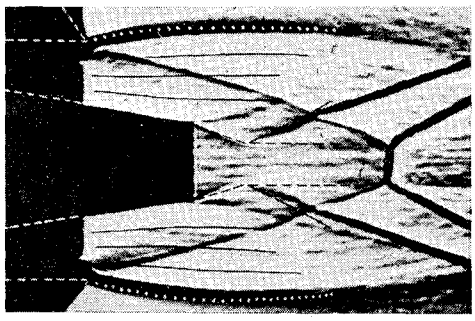

Fig. 11 Comparison of experimental and analytical flowfields for an axisymmetric internal-external-expansion *T-P* nozzle with $A_e/A_t = 1.555$, $L/L_{max} = 0.480$ and $P_a/P_{o1} = 0.136$.

Table 1 Comparison of experimental and analytical results for axisymmetric *T-P* nozzle[16]

L/L_{max}	$(P_b//P_{o1})_{exp}$	$(P_b/P_{o1})_{an}$
0.300	0.00346	0.00342
0.350	0.00385	0.00370
0.460	0.00365	0.00366

is presented in Table 1. In the absence of internal shock waves therefore, the analytical flow model produces results which agree quite well with measured values.

Conclusions

A technique is presented whereby the flowfields and base pressures of plug nozzles may be readily calculated. The solution includes an integral formulation of the near wake region which accurately describes the geometry of the near wake, and also predicts the pressure acting on the base of the plug. The use of the rotational method of characteristics provides the solution to the inviscid supersonic region adjacent to the near wake.

Parametric studies of the important plug nozzle variables are presented. Other data available for simpler base flow geometries indicate that the parameters studied do demonstrate the correct trends.

Comparisons between experimental geometries and the corresponding analytical model produced varied results. Base pressure agreement for large throat, large area ratio nozzles where no internal shock wave was present, appeared very satisfactory. However, for the small throat area low Mach number nozzle tested with an internal shock wave present, the analytical base pressure was about 26% higher. While this discrepancy was probably due in part to viscous effects and the use of a vertical sonic line, the internal shock wave appears to have the largest effect.

References

[1] Zumwalt, G. W., "Analytical and Experimental Study of the Axially-Symmetric Supersonic Base Pressure Problem," Ph.D. dissertation, 1959, Dept. of Mechanical Engineering, University of Illinois, Urbana, Ill.; also MIC 59-4589, University Microfilms, Inc., Ann Arbor, Michigan.

[2] Mueller, T. J., "Determination of the Turbulent Base Pressure in Supersonic Axisymmetric Flow," *Journal of Spacecraft and Rockets*, Vol. 5, No. 1, Jan. 1968, pp. 101–107.

[3] Mueller, T. J. and Hall, C. R., "Analytical Prediction of the Turbulent Base Pressure in Supersonic Axisymmetric Flow Including the Effect of Initial Flow Direction," AFFDL-TR-68-132, Sept. 1968, Air Force Flight Dynamics Lab. (AFSC) Wright-Patterson A.F.B., Ohio.

[4] Korst, H. H., Page, R. H. and Childs, M. E., "A Theory for Base Pressures in Transonic and Supersonic Flow," ME TN 392-2, May 1962, University of Illinois, Urbana, Ill.

[5] Zumwalt, G. W. and Tang, H. H., "Transient Base Pressure Study of an Axisymmetric Missile Flying Head-On Through a Blast Wave," Research Rept. SBW-6, Feb. 1964, School of Mechanical Engineering, Oklahoma State University, Stillwater, Okla.

[6] Hall, C. R., "An Analytical and Experimental Study of Non-Uniform Plug Nozzle Flow Fields," Ph.D. dissertation, Aug. 1970, Department of Aerospace and Mechanical Engineering, University of Notre Dame, Notre Dame, Ind.

[7] Channapragada, R. S., "Compressible Jet Spread Parameter for Mixing Zone Analyses," *AIAA Journal*, Vol. 1, No. 9, Sept. 1963, pp. 2188–2190.

[8] Golik, R. J., "On Dissipative Mechanisms Within Separated Flow Regions (With Special Consideration to Energy Transfer Across Turbulent, Compressible, $P_r = 1$, Mixing Regions)," Ph.D. dissertation, 1962, University of Illinois, Urbana, Ill.

[9] Hill, W. G., "Initial Development of Compressible Turbulent Free Shear Layers," Ph.D. dissertation, May 1966, Rutgers—The State University, New Brunswick, N.J.

[10] Carriere, P. and Sirieix, M., "Facteurs d'Influence du Receullement d'un Ecoulement Supersonique," *Proceedings of the 10th International Congress of Applied Mechanics*, Stresa, Italy, 1960.

[11] McDonald, H., "An Analysis of the Turbulent Base Pressure Problem in Supersonic Axisymmetric Flow," *The Aeronautical Quarterly*, Vol. XVI, May 1965, pp. 97–121.

[12] Korst, H. H., Chow, W. L. and Zumwalt, G. W., "Research on Transonic and Supersonic Flow of a Real Fluid at Abrupt Increases in Cross Section (With Special Consideration of Base Drag Problems)," ME TR 392-5, Oct. 1964, University of Illinois, Urbana, Ill.

[13] McDonald H. and Hughs, P. F., "A Correlation of High Subsonic Afterbody Drag in the Presence of a Propulsive Jet or Support Sting," *Journal of Aircraft*, Vol. 2, No. 3, May–June, 1965, pp. 202–207.

[14] Dixon, R. J. and Page, R. H., "Interdependence of Base Pressure and Base Heat Transfer," *ARS Journal*, Vol. 31, No. 12, Dec. 1961, pp. 1785–1786.

[15] Collines, D. J., Lees, L. and Roshko, A., "Near Wake of a Hypersonic Blunt Body with Mass Additions," *AIAA Journal*, Vol. 8, No. 5, May 1970, pp. 833–842.

[16] Mueller, T. J., United Aircraft Research Laboratory, East Hartford, Conn. 1965, unpublished data.

MAY 1972 J. SPACECRAFT VOL. 9, NO. 5

Material Phase Transformation Effects upon Performance of Spaced Bumper Systems

A. K. HOPKINS*
Air Force Materials Laboratory, Wright-Patterson Air Force Base, Ohio

T. W. LEE† AND H. F. SWIFT‡
University of Dayton Research Institute, Dayton, Ohio

The response of thin metal sheets to impacts by spheres of like materials in the entire velocity range to 7.2 km/sec is considered. Regimes of impact are observed characterized first by the projectile remaining intact, thence to projectile shatter, to melting of sphere and plate, and finally to vaporization of the materials. The thickness of witness plate material required to defeat the forward moving debris created by the thin plate impact is shown to depend on the physical state of the debris material. An analysis based upon planar shock wave theory is shown to accurately predict critical points on the ballistic limit curve associated with both incipient and complete melting and vaporization of the projectile and target materials.

Nomenclature

A, γ = coefficient and exponent for Murnaghan equation
E_H, P_H, V_H = Hugoniot energy, pressure, volume
E_0, V_0 = normal energy, volume
i = ith state or point
P^* = maximum shock pressure
s = spacing, cm
S = entropy, cal/°K
t_1, t_2 = thickness, cm
T = absolute temperature, °K
u_p = particle velocity in projectile, cm/μsec
u_T = particle velocity in target, cm/μsec
V^* = minimum volume
V_f = final volume, cm^3/g
v_0, v = impact velocity, km/sec
Γ = Grüneisen parameter

Introduction and Background

As early as 1947, Whipple[1] suggested that the most efficient method of defeating the penetrating power of a meteorite into the surface of a space vehicle is to provide the surface with a bumper. In his book published in 1958, Whipple[2] discusses the bumper concept in some detail, suggesting that over-all hull weight might be dramatically reduced by using the bumper concept.

Researchers since 1958 have developed the space bumper concept and have sought theoretical models which would explain the reason the bumper was effective and predict results of real impacts in space. In 1964 Maiden and McMillan[3] described the failure modes of bumper configurations at low and high velocity and suggested a one-dimensional analysis that would aid a space craft designer to estimate the bumper parameter values he would need in the construction of his vehicle.

In 1970, Swift and Hopkins[4] reported the effects of bumper materials upon the performance of two-component hypervelocity impact shields. They noted that most bumper materials performed equally well on a weight-per-unit-area basis, i.e., bumper areal density was the only factor controlling shield performance. This rule held exactly when one-dimensional shock wave analysis indicated that the projectiles (aluminum spheres) were melted by the primary shock wave and the bumper material also melted. Small deviations from the areal density rule were observed when the projectile melted, but the bumper material was neither vaporized nor shattered but left in the solid state. Shield performance degraded dramatically when the shock impedance of the bumper materials was insufficient to generate shock waves in the projectile strong enough to melt the projectile material—thus leaving the projectile material shattered but in the solid state. The authors hypothesized that the critical shock impedance of the bumper material needed to assure validity of

Received November 23, 1971; revision received January 18, 1972.
* Research Physicist.
† Head, Impact Physics Group.
‡ Head, Materials Physics Research.